

This is a repository copy of *Investigating defects and annual degradation in UK solar PV installations through thermographic and electroluminescent surveys*.

White Rose Research Online URL for this paper:

<https://eprints.whiterose.ac.uk/196697/>

Version: Published Version

Article:

Dhimish, Mahmoud and Badran, Ghadeer (2023) Investigating defects and annual degradation in UK solar PV installations through thermographic and electroluminescent surveys. *npj Materials Degradation*. 14. ISSN 2397-2106

<https://doi.org/10.1038/s41529-023-00331-y>

Reuse

This article is distributed under the terms of the Creative Commons Attribution (CC BY) licence. This licence allows you to distribute, remix, tweak, and build upon the work, even commercially, as long as you credit the authors for the original work. More information and the full terms of the licence here:

<https://creativecommons.org/licenses/>

Takedown

If you consider content in White Rose Research Online to be in breach of UK law, please notify us by emailing eprints@whiterose.ac.uk including the URL of the record and the reason for the withdrawal request.

ARTICLE OPEN



Investigating defects and annual degradation in UK solar PV installations through thermographic and electroluminescent surveys

Mahmoud Dhimish¹ and Ghadeer Badran¹

As the adoption of renewable energy sources, particularly photovoltaic (PV) solar, has increased, the need for effective inspection and data analytics techniques to detect early-stage defects, faults, and malfunctions has become critical for maintaining the reliability and efficiency of PV systems. In this study, we analysed thermal defects in 3.3 million PV modules located in the UK. Our findings show that 36.5% of all PV modules had thermal defects, with 900,000 displaying single or multiple hotspots and ~250,000 exhibiting heated substrings. We also observed an average temperature increase of 21.7 °C in defective PV modules. Additionally, two PV assets with 19.25 and 8.59% thermal defects were examined for PV degradation, and results revealed a higher degradation rate when more defects are present. These results demonstrate the importance of implementing cost-effective inspection procedures and data analytics platforms to extend the lifetime and improve the performance of PV systems.

npj Materials Degradation (2023)7:14; <https://doi.org/10.1038/s41529-023-00331-y>

INTRODUCTION

Over the past years, the UK has experienced exponential growth in solar photovoltaic (PV) deployment; for example, in January 2010, the UK had only 5735 PV installations, whereas according to the latest figures published by the UK government, end of August 2022, there is a total of 1,201,908 PV installations¹. This is an increase of 2.8% (387 MW) from August 2021. The majority of the newly installed PV systems last year were 4 kW, and 56% (7739 MW) of all PV installations in the UK have been ground-mounted or standalone. While solar capacity has increased, operation and maintenance of PV infrastructure have become more challenging. The level of power degradation in PV systems is not well understood, so this will be a unique investigation into the defects that prevail in these systems.

Previous papers, particularly in the UK, have reviewed the degradation of PV systems in the past couple of years. For example², has demonstrated that the annual mean degradation of over 7000 UK-based PV systems is near -0.8 to -0.9 /year. This is a very insightful result. However, in the same study, they studied the PV systems performance ratio (PR), which is a widely used metric^{3–5} for comparing the relative performance of PV systems whose design, technology and location differ. According to the study, the PR of UK systems is 83% with a standard deviation of 7%. This result suggests that possible failure modes and mismatching conditions are already present, and further investigation into this problem must be looked at.

Another recent study⁶ investigated the long-term PR ratio of PV systems that ran continuously from 2015 to 2019 in different countries across Europe. They have shown that the PR is 0.73 ± 0.08 in the Netherlands, Belgium, and Luxembourg, and 0.74 ± 0.08 in Germany. The outcome of this study indicates that PV systems have additional degradation while operating under field conditions, and this can suggest that there are existing defects that are happening without any “electrical” failure in the system. As such, PV installations can still generate power, but with additional losses/degradations. This problem is not easy to notice

purely by observing the output power data, particularly for MW PV assets, for the following reasons:

- (1) The inverter data precision is not ideal. Therefore, when data shows decrease in the output power, it can be sometimes assumed that the inverter, maximum power point (MPPT) unit^{7,8}, or the PV power optimiser⁹ is not 100% efficient.
- (2) To date, the existing PV degradation estimation models such as^{10,11} are not very accurate when all the PV-relevant parameters are unavailable. For example, the NREL model¹¹ requires the input of solar irradiance. At the same time, we understand that often the PV assets do not have Pyranometer or weather stations, and therefore, it would be necessary to acquire the solar irradiance for a national available database, which will result in an incorrect estimation of the actual degradation of the PV systems.
- (3) The variability and seasonality effect of PV power generation due to changes in the weather conditions. Climate change has contributed to rapid changes in pre-developed weather forecasting models; therefore, the weather nowadays is highly unpredictable. Many PV installers display that power loss is 5–10% due to this variability; hence, when PV power is decreased, unfortunately, it has been a common practice nowadays to suggest that this is due to the weather differences and no existing defects are currently encountering the PV assets! For example, a recent paper¹² proved that the overall error in the GB solar PV generation forecasting is $\pm 5.1\%$. Remarkably, this high error means that poor knowledge of the installed base of PV systems across the Great Britain is limited to the accuracy of the PV generation monitoring, and therefore existing PV forecasting models need to be further checked. Alternatively, this also suggests, for unknown reasons, that the actual performance of the PV installations usually has less performance than predicted.
- (4) In today's solar PV market, there is a wide range of PV module technologies, inverters, converters, and a wide

¹School of Physics, Engineering and Technology, University of York, York YO10 5DD, UK. ✉email: Mahmoud.dhimish@york.ac.uk

collection of power optimisers. This equipment and technological diversity contributed to further challenges in accurately predicting the actual performance of PV installations. For example, some PV technologies, such as Cadmium Telluride (CdTe)¹³, seem less efficient than silicon-based PV cells. Again, this mixture leads to the misconception that some PV assets have less output power production than others.

In the UK market and around the world, solar PV installations have grown exponentially. The use of fault detection algorithms and protection in PV installations is essential to prevent unexpected events¹⁴. In spite of the fact that these installations have few moving parts (in most cases) and typically require little maintenance, they may be subject to a variety of failures, including array disconnection, power conditioning units, wiring issues, and utility interconnection problems. Faults may be harder to detect in residential PV installations, and they can remain hidden until the whole system fails. There were a number of fire incidents reported in the media as a result of failure modes in PV installations. These fires are mostly caused by electrical arcing, or when there is an extreme temperature rise on the PV module surface, as in PV hotspots^{15–17}. These fires are also associated with defective bypass diodes^{18,19}.

PV industry concerns about potential induced degradation (PID) have only recently arisen. When electrons leak from the semiconductor material into other panel elements (such as frame and glass), current leakage occurs and power production is degraded^{20,21}. As a result of the PID, the PV modules' temperature rises rapidly (usually identified with aerial thermal inspections) and may cause the entire PV system to fail. The issue of PID can also occur in PV modules after a few months or years in the field. As of now, however, no predictive models have been developed for PID.

Cracks in solar cells are a common challenge! PV crack formation is inevitable during either the manufacturing or service life of the PV modules. In any case, it is currently unclear how to quantify its impact on PV performance. In addition, there is scant research examining whether cracks can accelerate the development of hotspots. Undetected cracks that were formed during production will result in a reduction of the expected service life of the PV modules²². Cracks are often invisible to the naked eye, and the current standard procedure is to detect them via EL imaging²³. They could lead to electrically disconnected cell regions, causing a decrease in short-circuit current and shunt resistance²⁴, subsequently reducing the module's power output²⁵. Cracks may also develop in the PV module if there are localised hotspots^{26,27}.

Therefore, the purpose of this research effort is to determine the actual performance of the UK's installed PV systems. Thus, the results of this study comprise over 2000 PV installations involving over 3,300,000 PV modules distributed throughout the UK. Our analysis aimed to address the following key questions: (1) what are the most prevalent hidden "deadly but silent" defects affecting UK PV assets, (2) what the actual PR ratio of these systems is, and (3) how well or poorly these different PV defects affect module performance.

RESULTS AND DISCUSSION

Data collection

This paper presents the output results of an evaluation of 3,300,000 PV modules located in the UK. PV systems have capacities ranging from 12 kW to 27 MW, and tilt angles range from 5° to 45°, while azimuth angles range from -70° (east) to +70° (west). It is important to note that we are not interested in assessing PV performance by location or distribution (components, inverters, etc.), but rather in breaking down the faults or defects that persist. It will provide a roadmap for further exploitation and work to be done in this research area by

identifying the gaps in understanding why some PV systems produce less power than others.

In order to analyse the defects and anomalies in the inspected PV modules, aerial thermography images were taken using a thermal drone. Most PV systems are examined using the EVO II Dual 640 T with Enterprise Bundle drone. A thermal camera has a sensitivity of 3 °C or 3% of the reading (whichever is greater). Solar irradiance was always above 500 W/m² during the summertime thermal inspection. Since this method of PV inspection does not require electrical disconnects of any of the PV systems, we chose it over electroluminescence (EL) inspection^{22,23}, which requires electrical disturbance of the system, or ultraviolet fluorescence (UVF) inspection²⁸, which does not identify all types of anomalies, such as PID.

Every PV installation under inspection was inspected for thermal anomalies, which were then classified into different categories. The current thermal inspection method cannot identify some PV defects, for example:

- (1) Every module affected by hotspots may not have cracks. Hence, hotspots in this paper only represent actual thermal hotspots identified in the modules, not necessarily real cracks or microcracks.
- (2) In some instances, Sometimes, problems with defective bypass diodes or soldering in the sub-strings can cause the same thermal images to be produced. If a single bypass diode is not functioning properly, a PV sub-string may become hotter than adjacent sub-strings with functioning bypass diodes. Therefore, in this study, a heated sub-string may indicate either inactive bypass diodes or soldering issues for PV module sub-strings. As it was not possible to obtain EL images of all the examined PV installations, this determination had to be made.

Two different examples of the thermal defects of PV assets are shown in Fig. 1. The red/yellow/blue dots represent the location of the thermal deficiency, which is identified and analysed using the thermal camera. For example, in Fig. 1a, A total of 4993 thermal defects were found in all 20,570 solar modules available for this PV asset (24.27% defective cases). Installation of this PV system is approximated at a title of 37° and a azimuth of -7°. Figure 2b shows our largest inspected solar asset, comprising 300,552 solar modules with 8563 thermal defects. PV modules in this installation have different azimuths (+13° to -25°) and titles (27° to 33°). Due to prior agreements with local authorities, the precise locations of PV assets are kept confidential.

A summary of PV defect categories/subcategories can be found in Fig. 1c. We analysed all PV system defects, including hotspots (Single HS or Multiple HS), heated substrings (Single HSS or Multiple HSS), PID, and heated junction boxes (HJB). To compare and analysed data, these defects were populated for each inspected PV installation.

PV thermal images

This section summarises the results of the thermal deficiencies in the inspected PV modules. For example, Fig. 2a, b shows a defective-free module and a PV module with a single HS, respectively. The thermal defect categorisation of several thousands of PV modules was also challenging; for example, in Fig. 2c, two or three solar cells and the junction box of the PV module have an elevated temperature. We, therefore, report such cases as "others" rather than classifying them into one of the identified PV deficiencies. Additionally, every thermal defect's median temperature was recorded; this will assist in determining how much temperature elevation has occurred in the different defects.

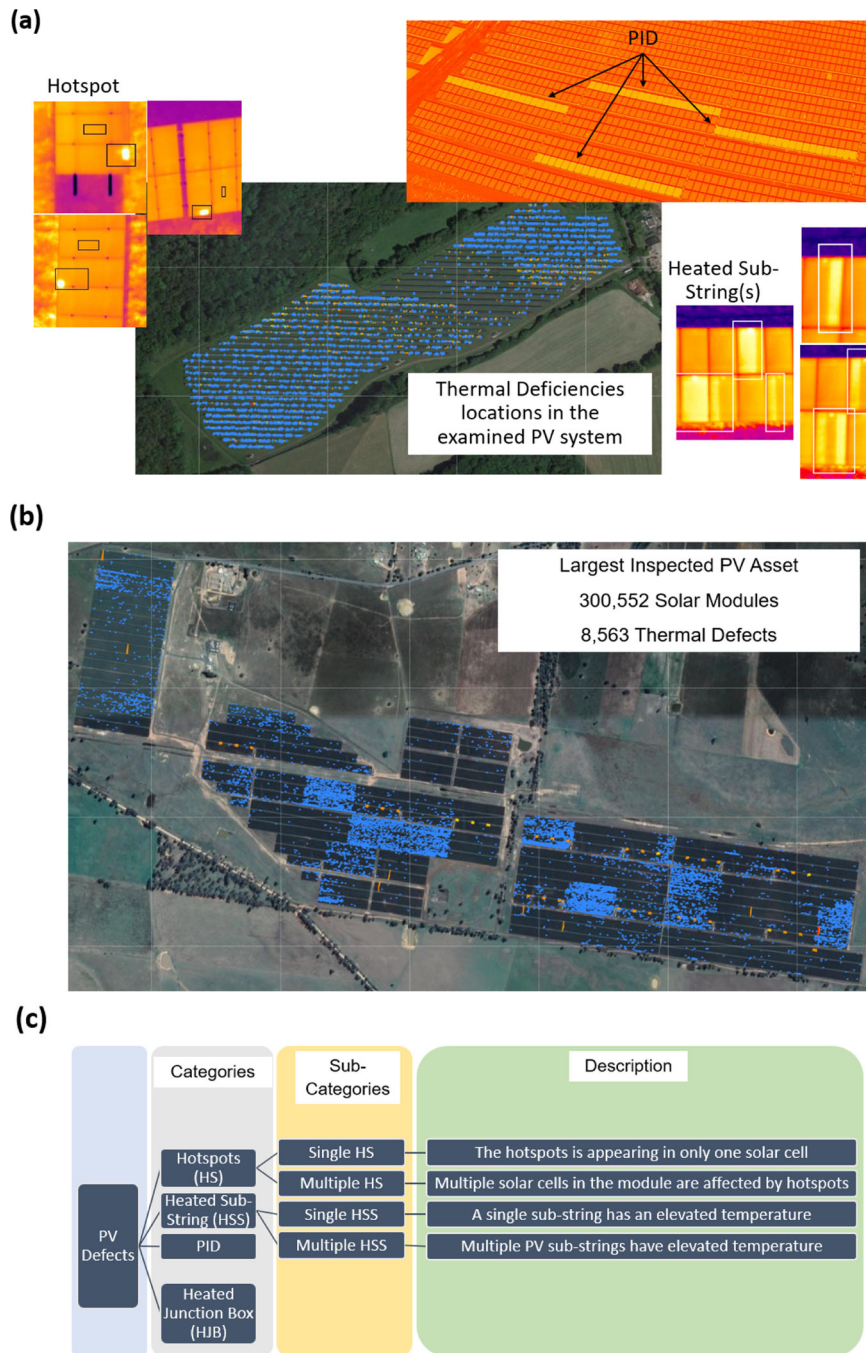


Fig. 1 Example of the analysis of the thermal efficiencies for two different PV assets. **a** A PV asset with 20,570 solar modules containing 4993 thermal defects. In this installation, hotspots, PIDs, and heated sub-strings are examples of thermal problems. Thermal defects are indicated by red, yellow, and blue dots. According to the “confidentiality agreement” with the PV asset owners, the precise geographical location of these assets is confidential. **b** Here is another example showing the locations where thermal anomalies were detected in one of the largest PV assets inspected, with 300,552 solar modules and 8563 thermal defects found. **c** Categories of the PV thermal anomalies investigated/analysed in this work.

Review of PV defects and temperature differences

A summary of all thermal defects found in inspected PV modules can be found in Fig. 3. According to the inspection, 36.6% of 3,300,000 modules were defective, while 63.4% were defect-free. As shown in Fig. 3a, with 512,612 reported cases, the single HS is the most common thermal defect. PID is the least common thermal fault; however, previous research^{29,30} has demonstrated that it can adversely affect PV modules and lead to 25–50% power losses. Compared with single HS, which are most likely to affect PV

modules with 5% power losses, PID can significantly impact PV module output power production.

According to Fig. 3b, 42.46% of all thermal defects are caused by a single HS, and 32.27% by multiple HS. A remarkable observation is that 16.5% of all faults are caused by one HSS. Consequently, defective bypass diodes or soldering defects are likely to cause PV module failures. A second interesting observation is that only 2.43% of PV modules are affected by an HJB. In light of recent papers³¹, it is surprising that this result emerged,

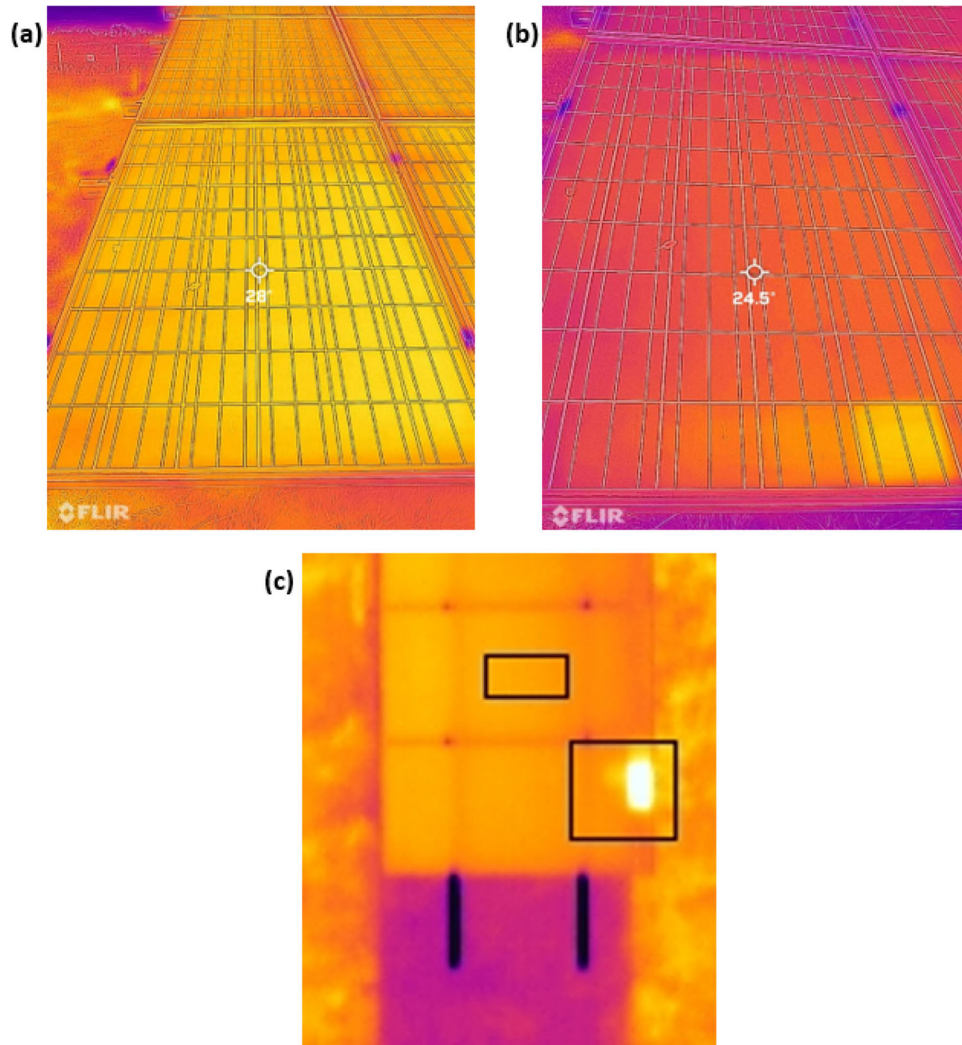


Fig. 2 Thermal image of PV modules. a Defective-free. **b** Single HS thermal defect. **c** Unclassified thermal defect on PV module (this could be HJB or multiple HS). These cases are reported as “others” in the thermal defect summary.

since it appears that HJBs constitute a significant problem faced by the solar PV industry today.

The temperature of every inspected PV module was recorded, and the difference between defective and defective-free solar cells were calculated using (1), ΔT . G_{STC} is the solar irradiance at standard test conditions, 1000 W/m^2 , and $G_{inspection}$ is the solar irradiance when the thermal image was taken. The ΔT_s represents the temperature with respect to the irradiance and calculated using (2). Where C_T is determined using (3) and presents the thermal dissipation coefficient under nominal operation solar cell temperature (NOCT), while I_c is the PV module current and V_D is the PV module voltage. S presents the surface area of the PV module:

$$\Delta T = \Delta T_s \frac{G_{STC}}{G_{inspection}} \quad (1)$$

$$\Delta T_s \approx C_T \times \frac{I_c \times V_D}{S} \quad (2)$$

$$C_T = \frac{\text{NOCT}(\text{measured in } ^\circ\text{C}) - 20}{800 \text{ W/m}^2} \quad (3)$$

For example, Fig. 4 shows two PV modules with recorded ΔT . For the upper PV module with no hotspots, the $\Delta T = 0.1^\circ\text{C}$, whereas the single HS in the lower PV module shows an elevated

temperature of $\Delta T = 26.3^\circ\text{C}$. The operating voltage loss, V_{loss} , of the PV module with $\Delta T = 0.1^\circ\text{C}$ is 0.03 V , and for the module with $\Delta T = 0.1^\circ\text{C}$ is equal to 30.7 V . The operating voltage of the thermally defective module is found using (4), where $V_{non-defective}$ and $V_{defective}$ represents the operating voltage of the adjacent non-defective PV module, and the module with thermal defect, respectively:

$$V_{loss} = V_{defective} - V_{non-defective} \quad (4)$$

Compare the mean and variation for data that has been collected under different conditions, typically after the ΔT calculation. Figure 5a plots the individual data values to look for differences in the centre line and the control limits (upper control limit (UCL) and lower control limit (LCL), which are calculated independently for each stage, to determine how ΔT changes. For all the considered thermal defects, the UCL is 30.0°C and the LCL is 13.5°C , and the mean value is 21.7°C . This result shows the significant temperature elevation for the PV modules affected by thermal defects.

The second plot, Fig. 5b, shows the boxplot, which can indicate the differences in the mean or variability of the data for the individual thermal defect. HJB has the most effect on the PV modules temperature, with averaged $\Delta T = 24.1^\circ\text{C}$, and the $\Delta T = 12.1^\circ\text{C}$ is observed from the PV modules affected by multiple HSS. It is

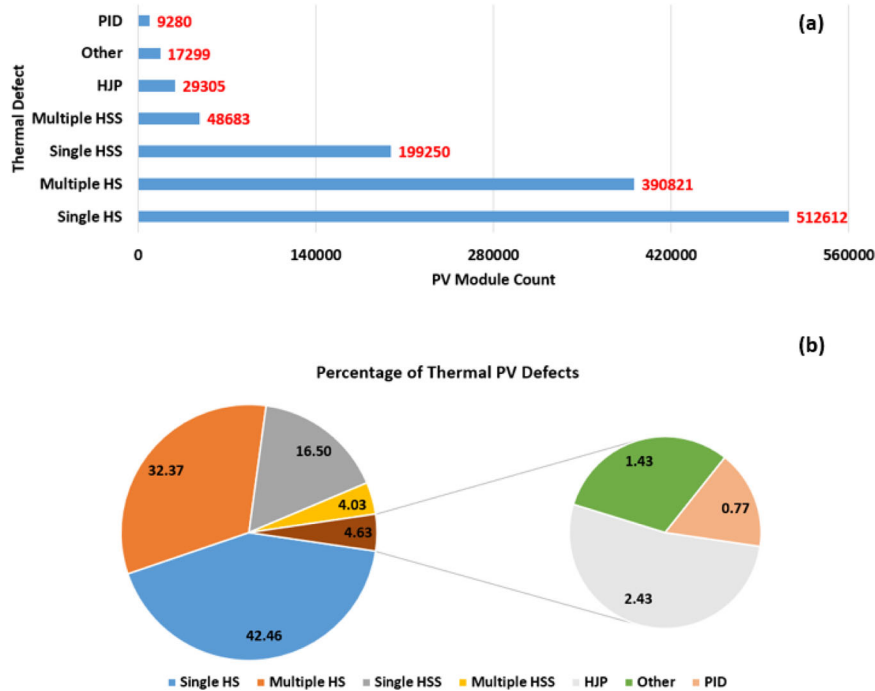


Fig. 3 Summary of the thermal efficiencies of the inspected PV modules. **a** PV count of thermal defects. **b** Percentage of PV defects.

interesting to notice that in almost all cases, there are some PV modules were operating under severe temperature levels $\Delta T > 50^\circ\text{C}$, which ultimately risks the PV system with a potential fire hazard.

It is worth mentioning that the ΔT results might contain a slight increase and variations because of the differences in the solar irradiation conditions when the thermal images were initially taken. However, results in Fig. 5 were plotted with a 95% confidence level and give an appropriate snapshot of how badly thermal defects can affect the PV modules surface temperature.

Thermal vs. electroluminescence investigation

In this section, we discuss the correlation between thermal and EL imaging for PV modules. Thermal images are known to aid in identifying PV faults^{32,33}, but EL images can also be used for determining solar cell health. Therefore, we have used an EL testing setup, as shown in Fig. 6 to test PV modules with different thermal defects.

The output thermal vs. EL images of the examined PV modules are shown in Fig. 7. The output thermal vs. EL images of the PV modules examined are shown in Fig. 7. In each case, the EL image intensity decreases (white represents high intensity, and black represents low intensity), indicating that the solar cell is affected by some anomaly:

- (1) According to Fig. 7a, a healthy PV module shows no anomalies the thermal image. The temperature is equally distributed across the surface of the PV modules, with $\Delta T \approx 0^\circ\text{C}$. Consequently, the EL image shows a uniform solar cell structure without any apparent defects/cracks/abnormalities.
- (2) The thermal image presented in Fig. 7b demonstrates a PV module with a heated sub-string with $\Delta T = 17.3 \pm 0.9^\circ\text{C}$. This heated sub-string is mainly due to a faulty bypass diode in the module. It is evident from the EL image that the affected sub-string exhibits no electroluminescent exposure (EL intensity is zero, complete black), providing a complete black-out (inactive) sub-string.
- (3) Figure 7c shows an example of a PV module with a PID with $\Delta T = 21.4 \pm 1.8^\circ\text{C}$. The EL image shows the low intensity of

almost all solar cells, which suggests that the PV module is badly affected by PID.

- (4) Finally, Fig. 7d presents the thermal and EL image of a PV module with a single hotspot, with $\Delta T = 28.7^\circ\text{C}$. The hot spotting problem is evident when examining the thermal image. However, there is no marker of defects when investigating the EL image. This is usually why thermal inspection, not EL, in such cases warrants PV hot spots.

Another comparative example of PV thermal vs. EL image is shown in Fig. 8. When observing the thermal image, no anomalies can be detected. However, almost all six PV modules developed cracks after completing the EL inspection. In addition, multiple solar cells exhibit low EL intensity, which could be due to early PID, shunting, or breakdown regions in the cells. As a result, the EL image assures that if these modules keep operating under field conditions, the cracks will deteriorate, creating hotspots, and thus reducing their power output.

This example illustrates the significance of conducting EL inspection on PV modules to observe any early-stage development of defects, cracks, shunting, etc., with the aim of assisting in proposing an early-stage prevention plan to overcome any possible future major breakdown in the modules.

PV degradation rate estimation: comparative assessment

This section demonstrates a comparative analysis of two utility-scale PV installations with a net capacity of 5 MW and 4.9 MW, both commissioned in January 2017. After thermal inspection, the first PV installation (PV installation #1) was found to have 4377 thermal defects (19.25%), whereas 1872 thermal defects (8.59%) were observed in the second PV installation (PV installation #2).

The output energy of both installations was analysed, and the PV degradation was estimated using NREL RdTools¹⁰. The PV degradation for PV installation #1 is equal to $-2.6 \pm 0.4\%$ /year, as shown in Fig. 9c. In comparison, in Fig. 9d, it is shown that the PV installation #2 has less annual PV degradation of $-1.2 \pm 0.2\%$ /year due to being affected by fewer defects. However, the degradation rate of both PV installations is higher than the UK degradation rate estimated previously by², with an average between -0.8% /year or

−0.9%/year. This comparison demonstrates the substantial effect of thermal defects on PV installation's yearly output power. Thus, thermal and EL inspection procedures must be considered, particularly for large-scale PV assets, to determine early-stage anomalies and prevent consequential future PV faults.

The evolution of thermal defects can accelerate year-to-year, as evidenced by a PV installation in Fig. 10a. The 5 MW PV installation was operational in March 2019, and the first inspection was

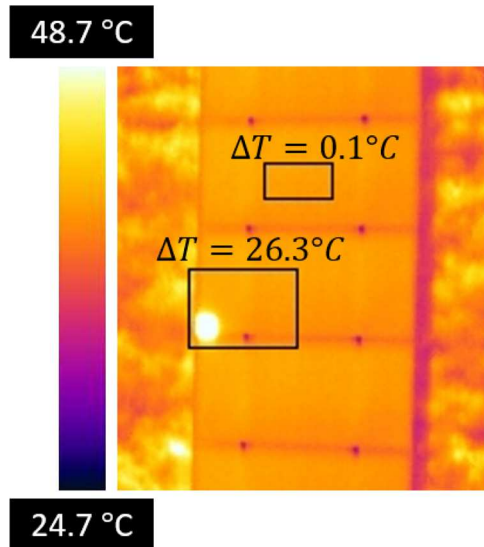


Fig. 4 An example of a thermal image taken for PV modules with different ΔT variations. In the example, we show that a PV module without hotspots has $\Delta T = 0.1^\circ\text{C}$ while it is equal to $\Delta T = 26.3^\circ\text{C}$ when a module is affected by a single HS.

completed in June 2019 to find 3.83% thermal defects. These defects grew to 7.48% in the following year. There were 8.31% and 10.03% thermal defects in June 2021 and 2022, respectively. The evolution of thermal anomalies in the system resulted in an additional degradation rate. Figure 10b shows the degradation rate estimation for the three years, 2020 to 2022; obviously, there needed to be more data samples to be analysed in June 2019 due to the PV system being operational for only 3-months since then.

The PV degradation is equal to $-2.56 \pm 0.3\%$ /year in June 2020, and for the subsequent years the degradation is $-2.71 \pm 0.2\%$ /year and $-3.32 \pm 0.3\%$ /year, in June 2021 and 2022, respectively. The data analysed for the degradation calculation was the “total” data gathered for the system. For example, in June 2021, the data used is the cumulation of the data samples taken from day one of operation until June 2021. This result demonstrates how severely the thermal defects affect PV energy generation and would subsequently impact the system with further degradation and reduce its life expectancy.

Summary of results

In summary, based on the analysis of 3.3 million PV modules distributed in multi-UK-based kW-to-MW PV installations, the outcome of their aerial thermography inspections is as follows:

- (1) A total of 36.6% of all PV modules inspected are thermally defective, while 63.4% are defect-free.
- (2) It has been found that over 900,000 PV modules have been affected by either single hotspots or multiple hotspots.
- (3) PID defects are found in 0.28% of PV modules inspected, resulting in 9280 defective panels. The module's performance can be severely affected by PID, with a drop in output power of 25 to 40%, compared, for example, with a slight decrease in output power when the module is affected by a hotspot (i.e., in some cases, there is a power drop of less than 1% from a single hotspot).

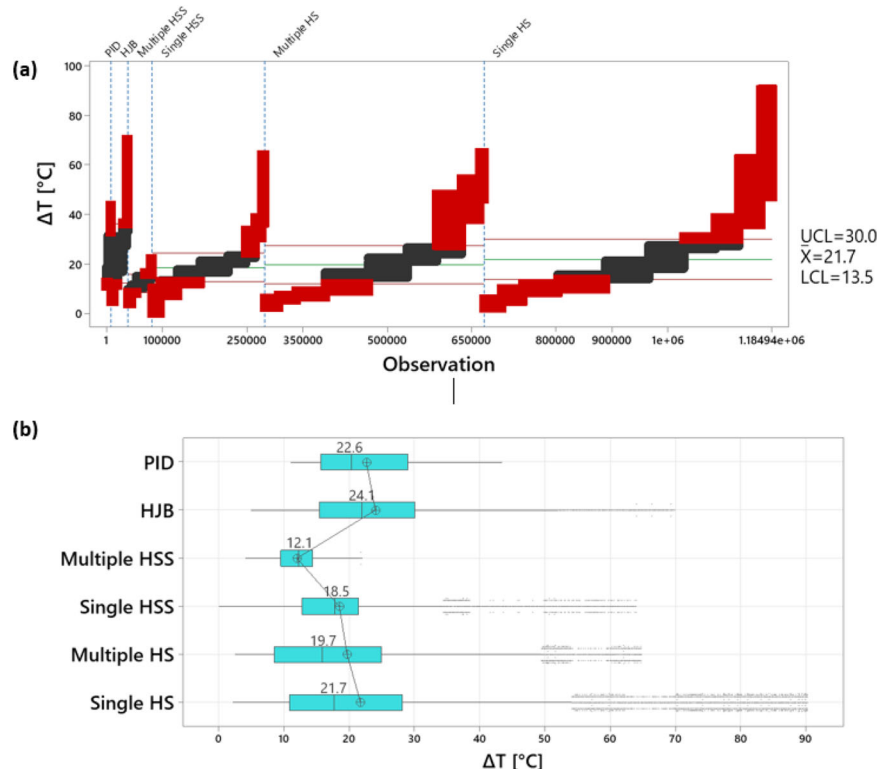


Fig. 5 Analysis of the datapoint of the temperature variations. **a** Distribution of all observations/samples vs. ΔT . **b** Boxplot of ΔT vs. explored thermal PV defects.

- (4) PV modules with thermal defects can have a higher surface temperature. In all inspected modules, the average difference between non-defective and defective modules is $21.7\text{ }^{\circ}\text{C}$, with some hotspots reaching $80\text{ }^{\circ}\text{C}$.



Fig. 6 EL imaging setup used to test the PV module. The EL camera is brought by Brightspot Automation, USA-based company.

- (5) The PV degradation of two PV installations with 19.25 and 8.59% thermal defects was investigated. When the PV asset is affected by higher thermal defects, it is found to have a higher degradation rate. In this industrial-relevant case study, we demonstrate that the first PV installation with higher thermal defects has an annual PV degradation rate of $-2.6 \pm 0.4\%$ /year compared with $-1.2 \pm 0.2\%$ /year for the second PV installation.
- (6) Finally, the year-to-year evolution of thermal defects in a PV installation with 18,867 PV modules has been demonstrated. In this case study, we show how thermal defects evolve in the modules over 4-years, with a system-level PV degradation rate starting at $-2.56 \pm 0.3\%$ /year in the first year and became $-3.32 \pm 0.3\%$ /year in last year.

In light of the above results, regular thermal inspection of PV installations is essential to prevent the accumulation of thermal defects and implement a recovery plan later. We also show in this paper that EL inspection can be used to identify “hidden” defects that are not yet fully apparent, such as thermal defects in modules.

Despite the discovery of these various thermal PV anomalies, there still needs to be an understanding of the behaviour and correlation between these defects in today’s solar PV industry. In other words, there is limited knowledge of how hotspots develop and why they change over time on solar cell and PV module levels. In addition, some previous research has explained the power losses associated with cracks in solar cells. However, there

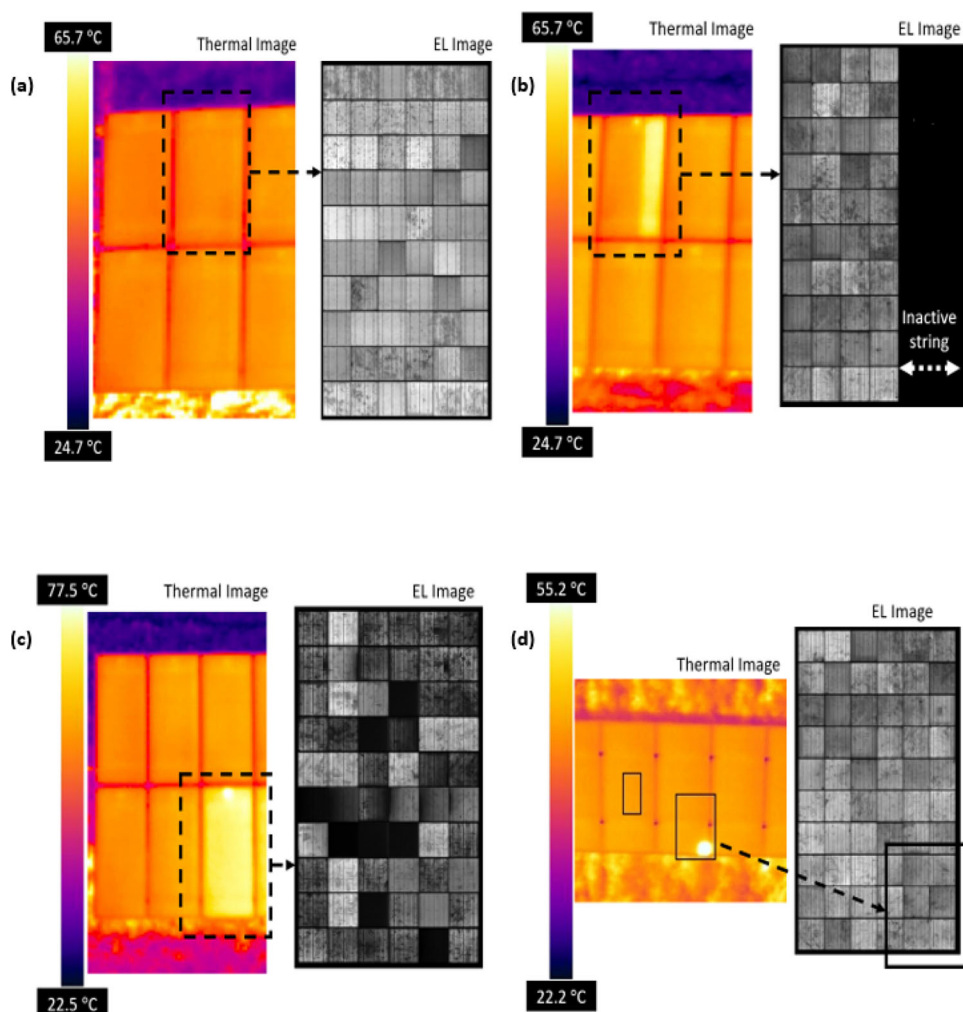


Fig. 7 Different examples of thermal vs. EL images of PV modules. **a** Defect-free PV module. **b** Inactive sub-string due to faulty bypass diode on PV module. **c** PV module is affected by PID. **d** PV module affected by single HS.

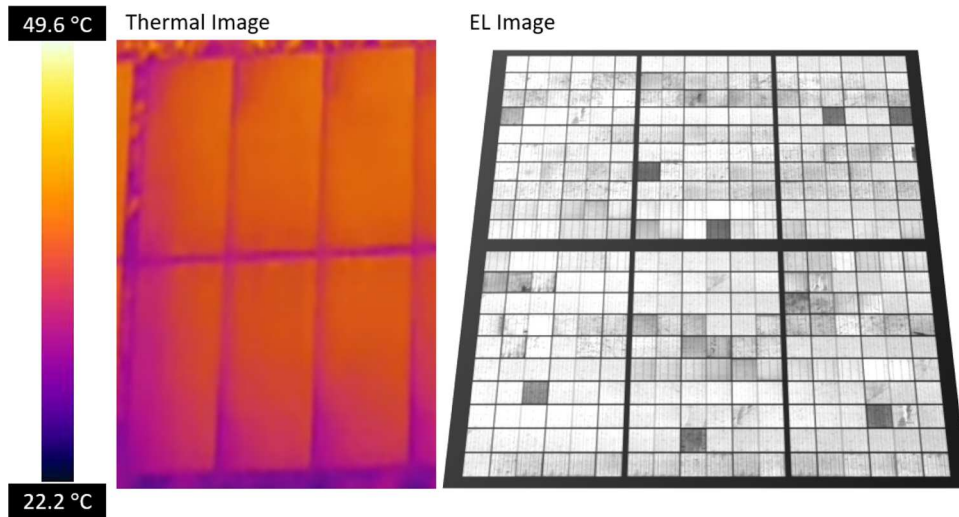


Fig. 8 Another two examples of thermal vs. EL images of PV modules. In spite of the fact that the EL images show that the PV modules have multiple cracks, there is no thermal defect in the modules (the solar cells are not becoming hotter).

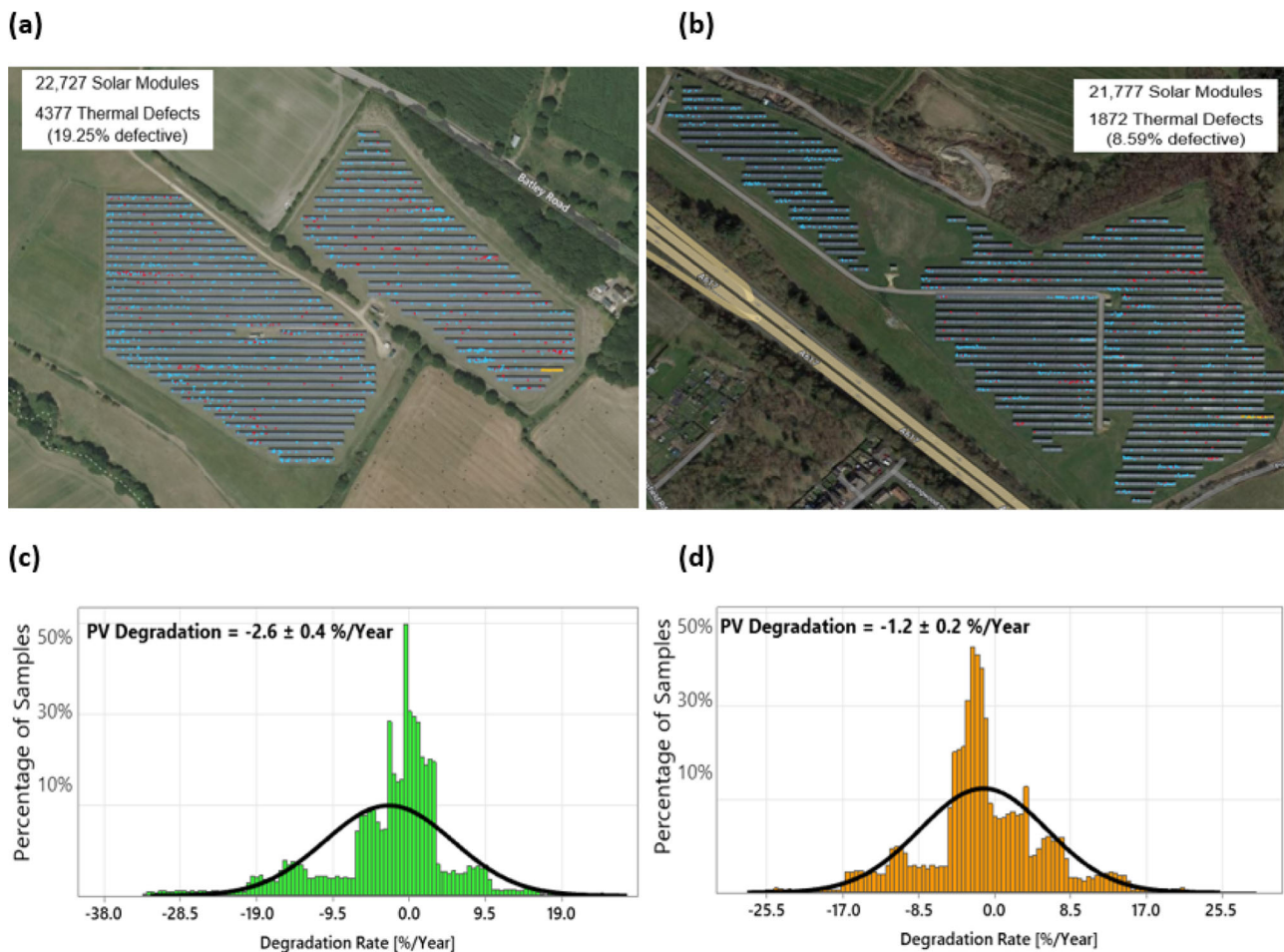


Fig. 9 A spotlight on two PV installations that have thermal defects. **a** A 5 MW PV installation with 19.25% thermal defects (referred to as PV installation 1). **b** A 4.9 MW PV installation with an identified thermal defect of 8.59% (known as PV installation #2). **c** Estimation of PV degradation for PV installation #1. **d** Estimation of PV degradation for PV installation #2. In January 2017, both PV installations went into operation after being constructed in 2016. A normal distribution fit curve (black curve in the histogram) shows the distribution of the samples.

is no scientific proof of whether hotspots can accelerate crack formation or the opposite. Likewise, PID can severely impact the performance of PV modules, and power losses can be as much as 40% for a typical PV array affected by PID. PID can be somewhat

mitigated using an anti-PID box installed between the PV array and the inverter. Again, however, there is no evidence that PID can cause or, at minimum, accelerate cracking, hotspots, or defective bypass diodes. These ideas are ideally to be further explored with

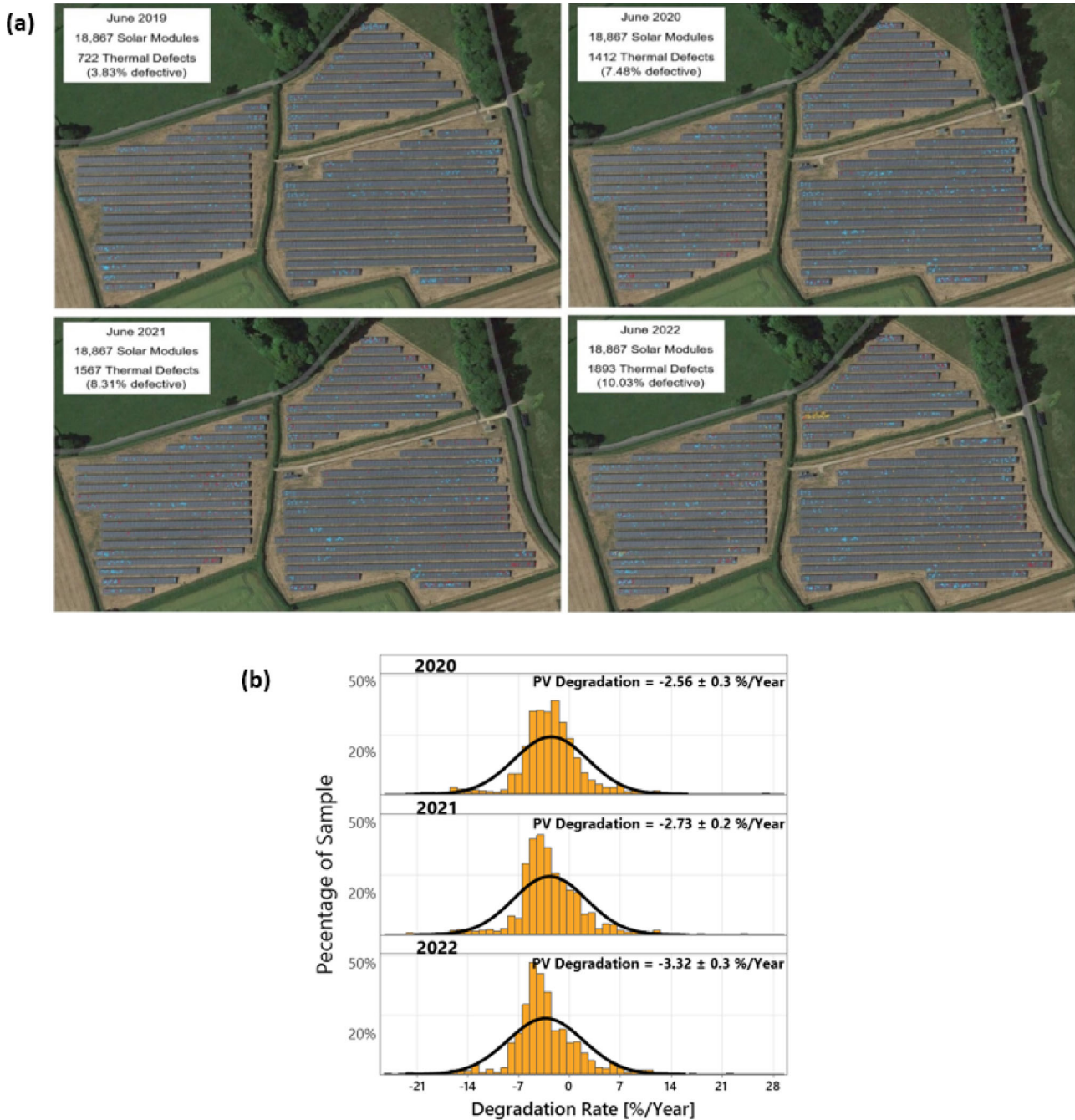


Fig. 10 Thermal defect evolution in a 5 MW PV installation. **a** Evolution of thermal defect locations over the period 2019–2022. **b** Estimated degradation rate for PV systems over time. The PV system consists of 18,867 solar modules and has been operational since March 2019. It took 3 months after the PV installations were commissioned to complete the first inspection, in June 2019.

indoor-and-outdoor experimental tests using different PV technologies, such as silicon, cadmium telluride, or perovskites.

METHODS

Thermal PV inspection

EVO II Dual 640T with Enterprise Bundle drone was used to conduct thermal inspections in this study. This drone is equipped with a dual-sensor thermal camera that can capture high-resolution thermal and visible light images and videos, making it well-suited for thermal inspection tasks. The Enterprise Bundle includes additional features and accessories that may enhance the

drone's capabilities, such as geofencing, automatic flight logs, and real-time video streaming. The EVO II Dual 640T with Enterprise Bundle is a professional-grade drone made by Autel Robotics. The 640T has a resolution of 640×512 pixels and a temperature range of -40 to 550 °C (-40 to 1022 °F).

EL PV inspection

BrightSpot Automation's Electroluminescence (EL) imaging technology is a method for inspecting photovoltaic (PV) modules in the field. EL imaging involves applying an electric current to a PV module and observing the emission of light from the material. This

can reveal defects or issues within the module that may not be visible using other inspection methods. Using EL imaging to inspect PV modules in the field can provide several advantages. It allows for the detection of subtle defects or issues that may not be visible using other inspection techniques and can be performed quickly and efficiently without the need for laboratory equipment. This can help identify issues with PV modules early on, allowing for timely repairs or maintenance to be carried out and helping to maximise the performance and efficiency of PV systems. Bright-Spot Automation's EL imaging technology is likely a valuable tool for professionals working in the PV industry, helping to ensure the reliability and performance of PV systems. An EL mirrorless camera with a CMOS sensor and a full-frame resolution of 6048 × 4024 pixels was used for this study. To ensure the highest quality EL images, the test time was fixed at 30 s, with a maximum exposure time of 30 s. The camera has 270 autofocus points and a 35 mm lens. The PV modules were tested under short-circuit current conditions using external power support. To minimise the impact of sunlight on EL transmission, all EL images were taken at night.

NREL RdTools

The National Renewable Energy Laboratory (NREL) RdTools is a software tool that is used to model and analyse the performance of photovoltaic (PV) systems. It is a user-friendly software that allows users to input data on PV system design and location, as well as weather data, to predict the performance of a PV system over its lifetime. RdTools can be used to optimise PV system design and determine the economic feasibility of PV projects. Some key features of NREL RdTools include:

- Performance prediction: RdTools can be used to predict the performance of PV systems under different weather conditions and over different periods of time. It considers factors such as solar irradiance, temperature, and shading to predict energy generation and system performance.
- System design optimisation: RdTools can be used to optimise the design of PV systems by helping users choose the most suitable PV modules, inverters, and other components based on their specific needs and goals.
- Data analysis and visualisation: RdTools includes a range of data analysis and visualisation tools that allow users to analyse and understand the performance of their PV systems in more depth.

DATA AVAILABILITY

The dataset generated and analysed in this study may be available from the corresponding author (M.D.) on reasonable request.

Received: 9 November 2022; Accepted: 9 February 2023;

Published online: 22 February 2023

REFERENCES

1. Department for Business, Energy and Industrial Strategy. Solar Photovoltaics deployment. GOV.UK. <https://www.gov.uk/government/statistics/solar-photovoltaics-deployment> (2022).
2. Taylor, J. et al. Performance of distributed PV in the UK: a statistical analysis of over 7000 systems. In *31st European Photovoltaic Solar Energy Conference and Exhibition (EU PVSEC 2015)*, 2263–2268 (2015).
3. Dhimish, M. & Tyrrell, A. M. Power loss and hotspot analysis for photovoltaic modules affected by potential induced degradation. *npj Mater. Degrad.* **6**, 11 (2022).
4. Lindig, S., Ascencio-Vasquez, J., Leloux, J., Moser, D. & Reinders, A. Performance analysis and degradation of a large fleet of PV Systems. *IEEE J. Photovolt.* **11**, 1312–1318 (2021).
5. Dhimish, M., Mather, P. & Holmes, V. Evaluating power loss and performance ratio of hot-spotted photovoltaic modules. *IEEE Trans. Electron Devices* **65**, 5419–5427 (2018).
6. Schardt, J. & te Heesen, H. Performance of roof-top PV systems in selected European countries from 2012 to 2019. *Sol. Energy* **217**, 235–244 (2021).
7. González-Castaño, C., Lorente-Leyva, L. L., Muñoz, J., Restrepo, C. & Peluffo-Ordóñez, D. H. An MPPT strategy based on a surface-based polynomial fitting for solar photovoltaic systems using real-time hardware. *Electronics* **10**, 206 (2021).
8. Yung Yap, K., Sarimuthu, C. R. & Mun-Yee Lim, J. Artificial intelligence based MPPT techniques for solar power system: a review. *J. Mod. Power Syst. Clean Energy* **8**, 1043–1059 (2020).
9. Gremmelpacher, J. M., Campamà Pizarro, R., van Jaarsveld, M., Davidsson, H. & Johansson, D. Historical building renovation and PV optimisation towards netzeb in Sweden. *Sol. Energy* **223**, 248–260 (2021).
10. John, J. J., Alnuaimi, A., Elnosh, A., Stefanchik, M. & Banda, P. Estimating degradation rates from 27 different PV modules installed in desert conditions using the NREL/rdtools. In *2018 IEEE 7th World Conference on Photovoltaic Energy Conversion (WCPEC) (A Joint Conference of 45th IEEE PVSC, 28th PVSEC & 34th EU PVSEC)*. <https://doi.org/10.1109/pvsc.2018.8547283> (2018).
11. Dhimish, M. Performance ratio and degradation rate analysis of 10-year field exposed residential photovoltaic installations in the UK and Ireland. *Clean Technol.* **2**, 170–183 (2020).
12. Huxley, O. T. et al. The uncertainties involved in measuring national solar photovoltaic electricity generation. *Renew. Sustain. Energy Rev.* **156**, 112000 (2022).
13. Dhimish, M., Schofield, N. & Attya, A. Insights on the degradation and performance of 3000 photovoltaic installations of various technologies across the United Kingdom. *IEEE Trans. Ind. Inform.* **17**, 5919–5926 (2021).
14. Aram, M., Zhang, X., Qi, D. & Ko, Y. A state-of-the-art review of fire safety of photovoltaic systems in buildings. *J. Clean. Prod.* **308**, 127239 (2021).
15. Nie, J., Luo, T. & Li, H. Automatic hotspots detection based on UAV infrared images for large-scale PV plant. *Electron. Lett.* **56**, 993–995 (2020).
16. Tang, S., Xing, Y., Chen, L., Song, X. & Yao, F. Review and a novel strategy for mitigating hot spot of PV panels. *Sol. Energy* **214**, 51–61 (2021).
17. Ma, M., Liu, H., Zhang, Z., Yun, P. & Liu, F. Rapid diagnosis of hot spot failure of crystalline silicon PV module based on I-V curve. *Microelectron. Reliab.* **100-101**, 113402 (2019).
18. Vieira, R., de Araújo, F., Dhimish, M. & Guerra, M. A comprehensive review on bypass diode application on photovoltaic modules. *Energies* **13**, 2472 (2020).
19. Xiao, C. et al. Failure analysis of field-failed bypass diodes. *Prog. Photovolt. Res. Appl.* **28**, 909–918 (2020).
20. Puranik, V. E. & Gupta, R. Novel quantitative electroluminescence method for detailed performance analysis of PID-S affected crystalline silicon PV module. *IEEE J. Photovolt.* **11**, 1470–1478 (2021).
21. Yamaguchi, S., Van Aken, B. B., Masuda, A. & Ohdaira, K. Potential-induced degradation in high-efficiency n-type crystalline-silicon photovoltaic modules: a literature review. *Sol. RRL* **5**, 2100708 (2021).
22. Dhimish, M., Ahmad, A. & Tyrrell, A. M. Inequalities in photovoltaics modules reliability: from packaging to PV Installation site. *Renew. Energy* **192**, 805–814 (2022).
23. Wang, Y. et al. Adaptive automatic solar cell defect detection and classification based on absolute electroluminescence imaging. *Energy* **229**, 120606 (2021).
24. Mohammed Niyaz, H., Meena, R. & Gupta, R. Impact of cracks on crystalline silicon photovoltaic modules temperature distribution. *Sol. Energy* **225**, 148–161 (2021).
25. Dhimish, M., d'Alessandro, V. & Daliento, S. Investigating the impact of cracks on solar cells performance: analysis based on nonuniform and uniform crack distributions. *IEEE Trans. Ind. Inform.* **18**, 1684–1693 (2022).
26. Lee, K., Cho, S., Yi, J. & Chang, H. Prediction of power output from a crystalline silicon photovoltaic module with repaired cell-in-hotspots. *Electronics* **11**, 2307 (2022).
27. Dhimish, M. & Lazaridis, P. I. An empirical investigation on the correlation between solar cell cracks and hotspots. *Sci. Rep.* **11**, 23961 (2021).
28. Kontges, M. et al. Review: Ultraviolet fluorescence as assessment tool for photovoltaic modules. *IEEE J. Photovolt.* **10**, 616–633 (2020).
29. Carolus, J. et al. Physics of potential-induced degradation in bifacial P-perc solar cells. *Sol. Energy Mater. Sol. Cells* **200**, 109950 (2019).
30. Xu, L. et al. Potential-induced degradation in perovskite/silicon tandem photovoltaic modules. *Cell Rep. Phys. Sci.* **3**, 101026 (2022).
31. Takashima, T. Behavior of interconnect-failed PV modules under standard test conditions and actual operation conditions. *IEEE J. Photovolt.* **8**, 1761–1766 (2018).
32. Ali, M. U., Khan, H. F., Masud, M., Kallu, K. D. & Zafar, A. A machine learning framework to identify the hotspot in photovoltaic module using infrared thermography. *Sol. Energy* **208**, 643–651 (2020).

33. Gallardo-Saavedra, S., Hernández-Callejo, L. & Duque-Perez, O. Technological Review of the instrumentation used in aerial thermographic inspection of photovoltaic plants. *Renew. Sustain. Energy Rev.* **93**, 566–579 (2018).

ACKNOWLEDGEMENTS

This work was supported by the EPSRC IAA (Project title: Next-Generation Vertically Mounted Bifacial Solar Panels: Conceptualisation, Field Testing, and Energy Performance Monitoring).

AUTHOR CONTRIBUTIONS

Both authors discussed the organisation and the content of the manuscript. M.D. and G.B. performed the experiments. M.D. prepared figures and wrote the original draft of the manuscript text. G.B. validated the experimental results and revised the manuscript. Both authors have approved the manuscript before submission.

COMPETING INTERESTS

The authors declare no competing interests.

ADDITIONAL INFORMATION

Correspondence and requests for materials should be addressed to Mahmoud Dhimish.

Reprints and permission information is available at <http://www.nature.com/reprints>

Publisher's note Springer Nature remains neutral with regard to jurisdictional claims in published maps and institutional affiliations.



Open Access This article is licensed under a Creative Commons Attribution 4.0 International License, which permits use, sharing, adaptation, distribution and reproduction in any medium or format, as long as you give appropriate credit to the original author(s) and the source, provide a link to the Creative Commons license, and indicate if changes were made. The images or other third party material in this article are included in the article's Creative Commons license, unless indicated otherwise in a credit line to the material. If material is not included in the article's Creative Commons license and your intended use is not permitted by statutory regulation or exceeds the permitted use, you will need to obtain permission directly from the copyright holder. To view a copy of this license, visit <http://creativecommons.org/licenses/by/4.0/>.

© The Author(s) 2023